



Highly Active Electrocatalysis of the Hydrogen Evolution Reaction by Cobalt Phosphide Nanoparticles**

Eric J. Popczun, Carlos G. Read, Christopher W. Roske, Nathan S. Lewis,* and Raymond E. Schaak*

Abstract: Nanoparticles of cobalt phosphide, CoP, have been prepared and evaluated as electrocatalysts for the hydrogen evolution reaction (HER) under strongly acidic conditions (0.50 M H_2SO_4 , pH 0.3). Uniform, multi-faceted CoP nanoparticles were synthesized by reacting Co nanoparticles with trioctylphosphine. Electrodes comprised of CoP nanoparticles on a Ti support (2 mg cm⁻² mass loading) produced a cathodic current density of 20 mA cm⁻² at an overpotential of -85 mV. The CoP/Ti electrodes were stable over 24 h of sustained hydrogen production in 0.50 M H_2SO_4 . The activity was essentially unchanged after 400 cyclic voltammetric sweeps, suggesting long-term viability under operating conditions. CoP is therefore amongst the most active, acid-stable, earth-abundant HER electrocatalysts reported to date.

The hydrogen evolution reaction (HER), which generates molecular hydrogen through the electrochemical reduction of water, underpins many clean-energy technologies. Platinum, the most widely used HER catalyst, requires very low overpotentials to generate large cathodic current densities in the highly acidic solutions that are used for water electrolysis in proton-exchange membrane systems.^[1–3] However, Pt is expensive and relatively scarce in the Earth's crust, limiting the utility of Pt in energy systems deployed at global scale. Active, acid-stable alternative HER electrocatalysts include the molybdenum-based MoS_2 ,^[2,4] MoB ,^[5] Mo_2C ,^[5,6] NiMoN_x ,^[7] and $\text{Co}_{0.6}\text{Mo}_{1.4}\text{N}_2$ ^[8] systems, as well as several first-row transition metal dichalcogenides.^[9] Alloys of Ni-Mo,^[10]

Ni-Mo-Zn,^[11] Ni-Fe,^[12] and Ni-P,^[13] along with Ni/NiO/CoSe₂ nanocomposites,^[14] are active HER electrocatalysts, but are not stable in acidic solutions.

Recently, nanoparticulate films of Ni₂P, comprised of inexpensive and earth-abundant elements, have been reported to show high HER activity, requiring an overpotential of -130 mV to produce cathodic current densities of 20 mA cm⁻² in 0.50 M H_2SO_4 .^[15] Like MoS_2 ,^[2,16] Ni₂P is also a hydrodesulfurization (HDS) catalyst,^[17,18] which suggests that other known HDS catalysts may also be active HER catalysts. We report herein that CoP, a known metal phosphide HDS catalyst that is structurally and compositionally distinct from Ni₂P,^[18] is a highly active and acid-stable HER catalyst, exhibiting an overpotential (η) of -85 mV at a current density (j) of -20 mA cm⁻² (at a mass loading of 2 mg cm⁻²), as well as stability over 24 h of operation in 0.50 M H_2SO_4 .

To synthesize the CoP nanoparticles, 9 ± 1 nm diameter spherical nanoparticles of ε-Co (Figure S1 in the Supporting Information) were prepared by the decomposition of [Co₂(CO)₈] in 1-octadecene (ODE), oleylamine (OLAM), and nonanoic acid (NA) at 230 °C, followed by addition of oleic acid (OLAC).^[19] To form CoP, the ε-Co nanoparticles were then reacted for 1 h at 320 °C with trioctylphosphine (TOP) in ODE and OLAM.^[20] (See Supporting Information for full experimental details.) Figure 1a and b show representative transmission electron microscope (TEM) images of the CoP nanoparticles, which were quasi-spherical, multi-faceted, uniform, and hollow, with an average diameter of 13 ± 2 nm. The hollow morphology is the result of a nanoscale Kirkendall effect, which often occurs for metal phosphide nanoparticles that have been synthesized by reaction of the metal nanoparticle templates with TOP.^[20–24]

Selected-area electron-diffraction (SAED) (Figure 1c) showed that the nanoparticles adopted the MnP structure type expected for CoP,^[25] whereas energy-dispersive X-ray spectroscopy (EDS) (Figure S2) indicated a 45:55 Co:P ratio, which is consistent within experimental error with the expected 1:1 stoichiometry of CoP. The powder X-ray diffraction (XRD) pattern (Figure 2a) confirmed that the bulk sample consisted of high-purity MnP-type CoP. Scherrer analysis of the peak widths of the XRD pattern for the CoP nanoparticles indicated an average grain size of 12 nm, which is consistent with the particle diameters observed by TEM, and suggests that the particles were largely single-crystalline. HRTEM (Figure 1d) confirmed that the CoP particles were single-crystalline, with observed lattice spacings of 2.4 Å that intersected in a manner consistent with expectations for the

[*] E. J. Popczun, C. G. Read,^[†] Prof. R. E. Schaak
Department of Chemistry and Materials Research Institute
The Pennsylvania State University
University Park, PA 16802 (USA)
E-mail: schaak@chem.psu.edu
C. W. Roske,^[†] Prof. N. S. Lewis
Division of Chemistry and Chemical Engineering
California Institute of Technology
Pasadena, CA 91125 (USA)
E-mail: nslewis@caltech.edu

[†] These authors contributed equally to this work.

[**] This work was supported by the National Science Foundation (NSF) Center for Chemical Innovation on Solar Fuels (CHE-1305124). C.W.R. thanks the NSF for a graduate research fellowship. Research was in part performed at the Beckman Institute Molecular Materials Research Center. TEM and BET data were acquired using facilities in the Materials Characterization Lab of the Penn State Materials Research Institute. E.J.P. and C.G.R. thank Trevor Clark, Ke Wang, and Lymanis Ortiz Rivera for assistance.

Supporting information for this article is available on the WWW under <http://dx.doi.org/10.1002/anie.201402646>.

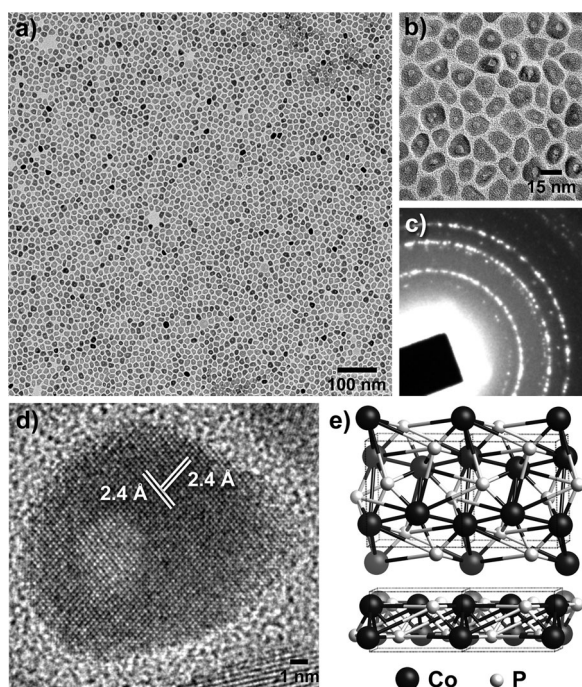


Figure 1. a, b) TEM images, c) SAED pattern, and d) HRTEM image of CoP nanoparticles. e) Two views of the MnP-type crystal structure of CoP.

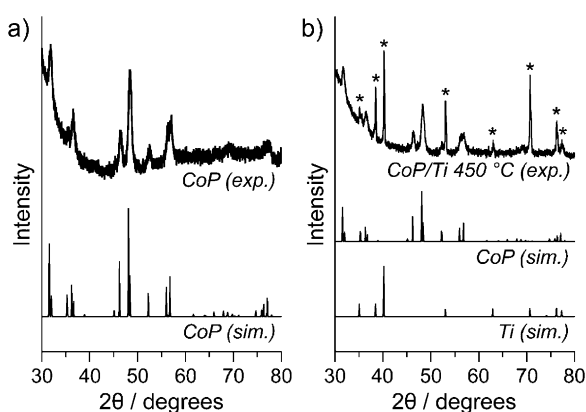


Figure 2. Powder XRD patterns for a) as-synthesized CoP nanoparticles (top, experimental; bottom, simulated) and b) a CoP/Ti electrode annealed at 450 °C (top, experimental; bottom, simulated for CoP and Ti). In (b), peaks marked with an asterisk (*) correspond to the Ti substrate.

closely spaced (102) and (111) planes of MnP-type CoP (Figure 1e).

The HER electrocatalytic activity of the CoP nanoparticles was evaluated in 0.50 M H_2SO_4 . Working electrodes were prepared by applying CoP nanoparticle samples to 0.2 cm^2 titanium supports with CoP loading densities of 0.9 and 2 mg cm^{-2} , respectively. Ti electrodes were chosen because Ti is not an active HER catalyst and because Ti promoted adhesion of the CoP nanoparticle catalysts, while remaining chemically inert. The CoP/Ti electrodes were heated at 450 °C in H_2/Ar to remove the organic ligands,

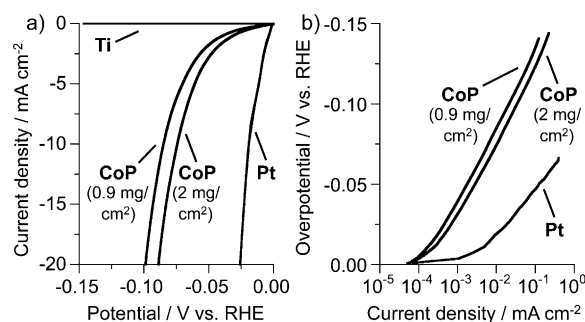


Figure 3. a) Polarization data in 0.50 M H_2SO_4 for CoP nanoparticle electrodes at mass loadings of 0.9 and 2 mg cm^{-2} , along with a Ti foil and Pt for comparison. b) Corresponding Tafel plots for the CoP and Pt electrodes.

and the powder XRD pattern (Figure 2b) confirmed that the nanocrystalline CoP phase persisted after this treatment. Figure 3a shows polarization data for representative CoP/Ti electrodes at two distinct mass loadings, along with polarization data obtained under identical conditions for uncoated Ti foil electrodes as well as for Pt, which is a benchmark HER electrocatalyst. Ten CoP/Ti electrodes, from several different CoP nanoparticle samples, were tested and showed highly consistent HER activities. The CoP nanoparticles produced a cathodic current density of 20 mA cm^{-2} at an overpotential of -95 mV for a mass loading of 0.9 mg cm^{-2} (i.e. $\eta_{-20 \text{ mA cm}^{-2}} = -95 \text{ mV}$) and exhibited $\eta_{-20 \text{ mA cm}^{-2}} = -85 \text{ mV}$ for a mass loading of 2 mg cm^{-2} . In contrast, the Ti foil electrode was not an active HER catalyst, as expected, under these conditions.

These overpotentials compare favorably to the values reported at similar current densities and mass loadings for other acid-stable, earth-abundant HER electrocatalysts, including Ni_2P ($\eta_{-20 \text{ mA cm}^{-2}} = -130 \text{ mV}$),^[15] Mo_2C on carbon nanotubes ($\eta_{-10 \text{ mA cm}^{-2}} = -152 \text{ mV}$),^[6] and MoS_2 ($\eta_{-20 \text{ mA cm}^{-2}} = -175 \text{ mV}$),^[4] and also compare favorably to, but are somewhat larger than, the behavior exhibited by the Pt control electrode ($\eta_{-20 \text{ mA cm}^{-2}} = -25 \text{ mV}$). The overpotentials exhibited by the CoP nanoparticles are also comparable to that of Ni-Mo nanopowder ($\eta_{-20 \text{ mA cm}^{-2}} = -80 \text{ mV}$),^[10] which is not stable under acidic conditions when Ni^{2+} is formed, and the $\eta_{-20 \text{ mA cm}^{-2}}$ for CoP is significantly smaller than $\eta_{-20 \text{ mA cm}^{-2}}$ for comparable catalytic systems that are unstable in acid, including Ni/NiO/CoSe₂ nanocomposites ($\eta_{-20 \text{ mA cm}^{-2}} \approx -120 \text{ mV}$).^[14] Porous nanosheets of isostructural FeP have been reported to catalyze the HER, but at significantly higher overpotentials ($\eta_{-20 \text{ mA cm}^{-2}} \approx -300 \text{ mV}$ for 0.28 mg cm^{-2} mass loading) than that of CoP, with unknown acid stability.^[26] Ni_5P_4 , as bulk pellets of nanocrystalline powders, also has been recently reported to be a highly active HER electrocatalyst in both acidic and alkaline solutions.^[27]

The slope of the Tafel plot [overpotential vs. log(cathodic current density)] for the Pt control (Figure 3b) was 30 mV/decade, which is consistent with that expected for the known HER mechanism on Pt. In contrast, the Tafel slope for representative CoP/Ti electrodes (Figure 3b) was 50 mV/decade, independent of mass loading. This value does not correspond to one of the standard HER Tafel slopes (29, 38, and 116 mV/decade),^[27] indicating that the mechanism of the

HER on CoP/Ti is different from that on Pt. The behavior of CoP is consistent with a mechanism in which the bond strength of the adsorbed hydrogen is sufficiently strong to provide an optimal coverage of the intermediate while not being so strong as to preclude desorption of the product. Similar Tafel slopes have been reported for other non noble-metal catalysts, such as MoS₂ (50 mV/decade),^[29] Mo₂C (55 mV/decade),^[29] and Ni₂P (46 mV/decade).^[15] The HER exchange current density of the CoP nanoparticle catalysts was $\approx 1.4 \times 10^{-4} \text{ A cm}^{-2}$, which is comparable to that exhibited by Ni₂P nanoparticles as HER electrocatalysts under acidic conditions.^[15]

To determine the faradaic yield for hydrogen evolution, a CoP/Ti working electrode was held at -20 mA cm^{-2} for 6.94 h. The amount of H₂ collected over 6.94 h was consistent with the amount of charge passed through the system (100 C), indicating essentially 100% faradaic efficiency for the HER. The amount of hydrogen produced also compared favorably with that produced by a Pt control cathode over the same time period. Complete decomposition of the catalyst would have produced gaseous byproducts that would account for less than 1% of the gas volume that was observed experimentally. This stable chemical behavior, coupled with the observed long-term acid stability of the material (confirming that significant degradation did not occur), therefore indicates that the CoP nanoparticle catalyst is capable of sustained electrocatalytic H₂ production in acidic media.

The CoP nanoparticles had a measured Brunauer–Emmett–Teller (BET) surface area of $59.1 \text{ m}^2 \text{ g}^{-1}$. Using this surface area, the turnover frequency (TOF) was calculated to be 0.046 s^{-1} at $\eta = 100 \text{ mV}$. As a benchmark, the upper limit of the surface area was estimated based on average particle geometry and size (e.g. 13 nm spheres) to be $71.9 \text{ m}^2 \text{ g}^{-1}$, and this procedure yielded a TOF of 0.038 s^{-1} . (See Supporting Information for detailed calculations.) These TOF values are estimates because the specific active sites are not known and because the calculations do not account for porosity or for surfaces that are inaccessible because of contacts between particles. However, the TOF values estimated based on both the experimental and theoretical surface areas are mutually comparable and compare favorably to the TOF values at $\eta = -100 \text{ mV}$ for Ni₂P nanoparticles (0.015 s^{-1}) and Ni–Mo nanopowder (0.05 s^{-1}).^[10,15]

To evaluate the stability of the CoP nanoparticles during repeated cycling in acidic solutions, accelerated degradation studies were performed on representative CoP/Ti electrodes having mass loadings of 0.9 mg cm^{-2} . As shown in Figure 4a, the CoP nanoparticles exhibited no measurable loss of activity after 400 cyclic voltammetry (CV) sweeps between +5 mV and -140 mV (vs. the reversible hydrogen electrode potential, RHE). The production of a current density of -20 mA cm^{-2} initially required an overpotential of -95 mV , whereas the overpotential changed to ca. -90 mV after 400 cycles, demonstrating high stability under strongly acidic conditions. In addition to the accelerated degradation studies, galvanostatic measurements at a current density of -20 mA cm^{-2} in a pre-electrolyzed solution indicated that the overpotential increased in magnitude only slightly (25 mV) over 24 h (Figure 4b) of continuous operation.

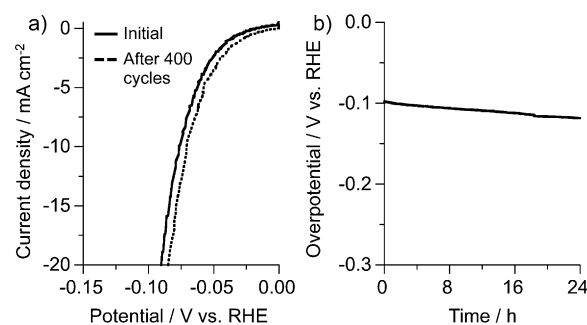


Figure 4. a) Polarization data in 0.50 M H₂SO₄ for a CoP/Ti electrode (0.2 mg cm^{-2} mass loading) initially and after 400 CV sweeps between +5 mV and -140 mV vs. RHE. b) Plot of overpotential vs. time for a CoP/Ti electrode (0.2 mg cm^{-2} mass loading) at a constant cathodic current density of 20 mA cm^{-2} .

Some particle desorption from the substrate (and therefore a slight decrease in mass loading) is the likely cause of this small increase in overpotential. Longer term stability measurements will require accelerated testing protocols that are currently being developed.

X-ray photoelectron spectroscopy (XPS) survey data (Figure S3) indicated that the surface of the as-prepared CoP/Ti electrode consisted primarily of carbon and oxygen, as expected from the organic surface-stabilizing agents. Co, P, and Ti were also present. After annealing the CoP/Ti electrode at 450°C , the carbon signal nearly disappeared, consistent with the expected removal of the capping ligands. High-resolution XPS data for the annealed CoP/Ti electrode showed two characteristic Co 2p peaks, with binding energies consistent with those expected for Co^{II}. Following electrolysis, additional sulfur, carbon, and nitrogen were present, with these signals attributable to the sulfuric acid electrolyte, the graphite rod counter electrode, and epoxy, respectively. Oxygen was present throughout, which was expected due to the handling of samples in air. Importantly, XPS confirmed that the electrode was free of trace Pt, indicating that the observed HER activity was primarily due to the CoP nanoparticles and not to adventitious noble metal impurities.

In conclusion, nanoparticles of CoP are highly active HER electrocatalysts, with $< 100 \text{ mV}$ overpotentials at low mass loadings and operationally relevant current densities of -20 mA cm^{-2} . Sensitivity analyses of a complete solar fuels generator system are required to ascertain quantitatively the remaining gains in system efficiency associated with a further reduction in the overpotential for the HER, as compared to improvements in the performance of the other key components of such a full system. In addition, CoP nanoparticles are exceptionally stable in acidic solutions, showing no evidence of significant degradation over 24 h of H₂ production in 0.50 M H₂SO₄. These results further establish that HDS electrocatalysts comprised of inexpensive and earth-abundant elements provide interesting and important candidate materials for obtaining high activity and stability for the HER in acidic media.

Received: February 20, 2014

Published online: April 11, 2014

Keywords: electrocatalysis · hydrogen evolution · metal phosphide · nanomaterials · water splitting

-
- [1] H. B. Gray, *Nat. Chem.* **2009**, *1*, 112.
 [2] D. Merki, X. Hu, *Energy Environ. Sci.* **2011**, *4*, 3878.
 [3] M. G. Walter, E. L. Warren, J. R. McKone, S. W. Boettcher, Q. Mi, E. A. Santori, N. S. Lewis, *Chem. Rev.* **2010**, *110*, 6446.
 [4] Y. Li, H. Wang, L. Xie, Y. Liang, G. Hong, H. Dai, *J. Am. Chem. Soc.* **2011**, *133*, 7296.
 [5] H. Vrubel, X. Hu, *Angew. Chem.* **2012**, *124*, 12875–12878; *Angew. Chem. Int. Ed.* **2012**, *51*, 12703–12706.
 [6] W.-F. Chen, C. H. Wang, K. Sasaki, N. Marinkovic, W. Xu, J. T. Muckerman, Y. Zhu, R. R. Adzic, *Energy Environ. Sci.* **2013**, *6*, 943.
 [7] W.-F. Chen, K. Sasaki, C. Ma, A. I. Frenkel, N. Marinkovic, J. T. Muckerman, Y. Zhu, R. R. Adzic, *Angew. Chem.* **2012**, *124*, 6235; *Angew. Chem. Int. Ed.* **2012**, *51*, 6131.
 [8] B. Cao, G. M. Veith, J. C. Neufeld, R. R. Adzic, P. G. Khalifah, *J. Am. Chem. Soc.* **2013**, *135*, 19186.
 [9] D. Kong, J. J. Cha, H. Wang, H. R. Lee, Y. Cui, *Energy Environ. Sci.* **2013**, *6*, 3553.
 [10] J. R. McKone, B. F. Sadtler, C. A. Werlang, N. S. Lewis, H. B. Gray, *ACS Catal.* **2013**, *3*, 166.
 [11] D. G. Nocera, *Acc. Chem. Res.* **2012**, *45*, 767.
 [12] I. A. Raj, K. I. Vasu, *J. Appl. Electrochem.* **1990**, *20*, 32.
 [13] I. Paseka, *Electrochim. Acta* **1995**, *40*, 1633.
 [14] Y. F. Xu, M. R. Gao, Y. R. Zheng, J. Jiang, S. H. Yu, *Angew. Chem.* **2013**, *125*, 8708; *Angew. Chem. Int. Ed.* **2013**, *52*, 8546.
 [15] E. J. Popczun, J. R. McKone, C. G. Read, A. J. Biacchi, A. M. Wilttrout, N. S. Lewis, R. E. Schaak, *J. Am. Chem. Soc.* **2013**, *135*, 9267.
 [16] R. Prins, V. H. J. De Beer, G. A. Somorjai, *Catal. Rev.* **1989**, *31*, 1.
 [17] P. Liu, J. A. Rodriguez, T. Asakura, J. O. Gomes, K. Nakamura, *J. Phys. Chem. B* **2005**, *109*, 4575.
 [18] S. T. Oyama, *J. Catal.* **2003**, *216*, 343.
 [19] S. Deka, A. Falqui, G. Berton, C. Sangregorio, G. Ponetti, G. Morello, M. D. Giorgi, C. Giannini, R. Cingolani, L. Manna, P. D. Cozzoli, *J. Am. Chem. Soc.* **2009**, *131*, 12817.
 [20] D.-H. Ha, L. M. Moreau, C. R. Bealing, H. Zhang, R. G. Hennig, R. D. Robinson, *J. Mater. Chem.* **2011**, *21*, 11498.
 [21] R.-K. Chiang, R.-T. Chiang, *Inorg. Chem.* **2007**, *46*, 369.
 [22] J. Wang, A. C. Johnston-Peck, J. B. Tracy, *Chem. Mater.* **2009**, *21*, 4462.
 [23] A. E. Henkes, Y. Vasquez, R. E. Schaak, *J. Am. Chem. Soc.* **2007**, *129*, 1896.
 [24] E. Muthuswamy, S. L. Brock, *Chem. Commun.* **2011**, *47*, 12334.
 [25] S. Rundqvist, *Acta Chem. Scand.* **1962**, *16*, 287.
 [26] Y. Xu, R. Wu, J. Zhang, Y. Shi, B. Zhang, *Chem. Commun.* **2013**, *49*, 6656.
 [27] A. B. Laursen, K. R. Patraju, M. J. Whitaker, M. Retuerto, T. Sarkar, N. Yao, K. V. Ramanujachary, M. Greenblatt, G. C. Dismukes, personal communication.
 [28] J. O. M. Bockris, E. C. Potter, *J. Electrochem. Soc.* **1952**, *99*, 169.
 [29] J. Kibsgaard, Z. Chen, B. N. Reinecke, T. F. Jaramillo, *Nat. Mater.* **2012**, *11*, 963.
-